

Reliable Label Correction is a Good Booster When Learning with Extremely Noisy Labels

Kai Wang^{*1} Xiangyu Peng^{*1} Shuo Yang² Jianfei Yang³ Zheng Zhu⁴ Xinchao Wang¹ Yang You¹
 Code: <https://github.com/xyupeng/LC-Booster>

Abstract

Learning with noisy labels has aroused much research interest since data annotations, especially for large-scale datasets, may be inevitably imperfect. Recent approaches resort to a semi-supervised learning problem by dividing training samples into clean and noisy sets. This paradigm, however, is prone to significant degeneration under heavy label noise, as the number of clean samples is too small for conventional methods to behave well. In this paper, we introduce a novel framework, termed as LC-Booster, to explicitly tackle learning under extreme noise. The core idea of LC-Booster is to incorporate label correction into the sample selection, so that more purified samples, through the reliable label correction, can be utilized for training, thereby alleviating the confirmation bias. Experiments show that LC-Booster advances state-of-the-art results on several noisy-label benchmarks, including CIFAR-10, CIFAR-100, Clothing1M and WebVision. Remarkably, under the extreme 90% noise ratio, LC-Booster achieves 93.5% and 48.4% accuracy on CIFAR-10 and CIFAR-100, surpassing the state-of-the-art by 1.6% and 7.2% respectively.

1. Introduction

Contemporary large-scale datasets are prone to be contaminated by noisy labels, due to inevitable human failure, unreliable open-source tags (Mahajan et al., 2018), challenging labeling tasks (Frénay & Verleysen, 2013), and errors made by machine generation (Kuznetsova et al., 2020). Training deep neural networks (DNNs) with a non-trivial amount of label noise could result in poor generalization performance (Zhang et al., 2017a). This behavior can be explained

^{*}Equal contribution ¹National University of Singapore ²University of Technology Sydney ³Nanyang Technological University ⁴Tsinghua University. Correspondence to: Yang You <youyou@comp.nus.edu.sg>.

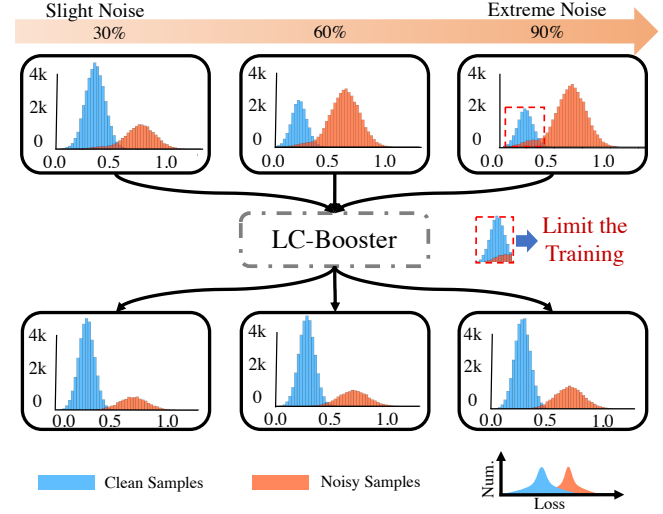


Figure 1. The motivation of the proposed LC-Booster. From left to right, the noise ratio increases from 30% to 90%. The histograms show normalized losses used to divide clean and noisy sets based on Gaussian Mixture Model (GMM). Conventionally, the number of clean samples shrinks significantly as noise ratio rises (the top row), which may limit the training of models. In this work, we find that noisy labels could be reliably revised in the sample selection setting (the bottom row), so that more purified clean samples could be involved in training to boost model performance.

by the over-parameterization characteristics of DNN (Allen-Zhu et al., 2018) and the consequent strong memorization ability (Arpit et al., 2017).

Recently, a variety of approaches have been proposed to train robust DNNs in a noisy label environment. Some of the works adopt label correction to revise noisy labels based on network predictions (Wang et al., 2020; Wu et al., 2020), thus reducing the noise level in the dataset. However, these methods may suffer from the accumulation of prediction errors in the process of re-labeling, which is also known as confirmation bias (Arazo et al., 2020). More recently, a series of works based on sample selection (SS) stand out and show promising results. The main idea is to distill clean samples from noisy data for training so that the negative influence of label noise could be mitigated. Among these meth-

ods, Co-teaching (Han et al., 2018) and Co-teaching+ (Yu et al., 2019) select a portion of small-loss instances as clean samples since DNNs tend to learn easy and clean samples first before overfitting to noisy labels (Arpit et al., 2017). Another representative work DivideMix (Li et al., 2020) fits a Gaussian Mixture Model (GMM) on the per-sample loss distribution for adaptive sample selection. To avoid confirmation bias, it adopts a two-network structure where the GMM for one network is used to divide training data for the other network.

Though SS-based methods can effectively pick out most of the clean samples, their performance would degenerate significantly when confronting extremely noisy labels. This can be easily understood, as the size of the clean set is intrinsically limited by the true number of clean samples in the given noisy dataset, even if all clean samples can be precisely picked out in the ideal case. Also, training with such a small labeled set may lead to biased or insufficiently trained models and consequent poor generalization performance. This naturally raises a question: Is it possible to enlarge the clean set for further performance-boosting, on top of filtering out adverse noisy labels?

To answer this question, we first identify that sample selection based methods intrinsically lack a mechanism to produce new clean samples, despite their excellent ability to distill a much clean set from large label noise. This inspires us that an extra technique is necessary to achieve it. To this end, we rethink the feasibility of label correction, a conventional tool to turn noisy samples into clean ones, in the new setting of sample selection. Previous label correction methods, as mentioned above, are prone to suffer from confirmation bias, since model predictions could be severely hurt when heavy label noise is involved in training. However, in the SS setting, the problem of confirmation bias could be largely mitigated, as much label noise is filtered out and only a highly purified clean set is used for supervised training. Based on the trusted clean set, predictions of the model are much more reliable sources for label correction. In fact, attempts have been made to increase the reliability of label correction. (Reed et al., 2014) use bootstrapping to generate new labels. (Zhang et al., 2020) leverage a side clean set (*i.e.*, clean samples given in advance) as anchors to reconstruct the noisy dataset. However, we argue that neither bootstrapping nor anchor clean samples are necessary, as in the SS setting a trusted clean set is naturally provided which label correction could rely on.

Based on this insight, we propose LC-Booster, a noise-robust framework that leverages label correction jointly with sample selection for a performance boost. In this framework, the clean set could keep a high label precision with adaptive sample selection while extending its size thanks to reliable label correction. Specifically, we start by warming up the

model for a few iterations, so that some easy patterns can be learned first. Then, we divide clean and noisy samples based on GMM loss modeling as in (Li et al., 2020), where labels of the clean samples are kept for supervised loss and noisy samples are treated in an unsupervised manner. For better generalization, we also adopt a hybrid augmentation (H-Aug.) strategy that enforces consistency on both weak-weak and weak-strong augmented views. At around the middle stage, Reliable Label Correction (ReCo) is adopted to revise the labels for both clean and noisy samples. We theoretically show that the precision of revised labels can be guaranteed with a proper choice of threshold. With ReCo involved in training, the clean set can be improved in terms of both purity and quantity (shown at the bottom of Fig. 1), which could guide the model to learn better representations.

To the best of our knowledge, we are the first to leverage the strengths of both sample selection and label correction in a unified framework, despite the simplicity of the individual technique. We validate the effectiveness of LC-Booster on several noisy-label benchmarks, including CIFAR-10, CIFAR-100, Clothing1M, and WebVision. Our approach achieves state-of-the-art results on most of these datasets. Remarkably, under the extreme 90% noise ratio, our approach achieves 93.5% and 48.4% accuracy on CIFAR-10 and CIFAR-100, surpassing the previous best by 1.6% and 7.2% respectively. Our main contributions can be summarized as:

- We find that label correction can be naturally leveraged with sample selection as a new paradigm for learning with noisy labels. The two techniques could work jointly to make a larger and more purified clean set.
- We propose LC-Booster, a simple yet efficient framework that could boost performance under (extreme) label noise. LC-Booster adopts H-Aug. for better generalization and ReCo for precisely revising labels with backing up theorem.
- We experimentally show that LC-Booster advances state-of-the-art results on multiple benchmarks, especially under heavy label noise. We also conduct extensive ablation studies to illustrate the effects of our method.

2. Preliminaries

2.1. Problem Formulation

In the problem of learning with noisy labels (LNL), we consider the noisy training set $\mathcal{S} = \{(\mathbf{x}_i, \tilde{\mathbf{y}}_i)\}_{i=1}^N = (\mathcal{S}_x, \mathcal{S}_{\tilde{y}})$, where \mathbf{x}_i is the i^{th} image and $\tilde{\mathbf{y}}_i \in \{0, 1\}^C$ is the one-hot label over C classes. $(\mathbf{x}_i, \tilde{\mathbf{y}}_i)$ is an image-target pair drawn from random variables $(X, \tilde{Y}) \sim (\mathcal{D}_X, \mathcal{D}_{\tilde{Y}})$, where \mathcal{D}_X and $\mathcal{D}_{\tilde{Y}}$ denote the data distribution and the noisy label

distribution, respectively. Similarly, we use $Y \sim \mathcal{D}_Y$ to represent the distribution for ground truth labels, which is unknown in the LNL problem setting. The noise rate of given class c is defined as $\rho_c = P(\tilde{Y} = e_c | Y \neq e_c)$, with e_c denoting the one-hot vector activated in position c , and the overall noise rate is $\rho = \frac{1}{C} \sum_{i=1}^C P(\tilde{Y} = e_i | Y \neq e_i)$. Generally, \tilde{Y} can be divided into two types:

- Symmetric noise \tilde{Y}_{sym} . The label flips to a random class with a fixed probability η . With symmetric noise, we have $P(\tilde{Y}_{sym} = e_i | Y = e_i) = 1 - \eta + \frac{\eta}{C}$ and $P(\tilde{Y}_{sym} = e_j | Y = e_i) = \frac{\eta}{C}, \forall i, j \in \{1, 2, \dots, C\}, i \neq j$.
- Asymmetric noise \tilde{Y}_{asym} . The label flips to a certain class defined in a dictionary \mathcal{M} , which is built on the mapping between similar classes, *i.e.*, $cat \rightarrow dog$, $deer \rightarrow horse$, $bird \rightarrow airplane$. With flipping probability η , we can arrive at $P(\tilde{Y}_{asym} = e_i | Y = e_i) = 1 - \eta + \mathbb{1}_{\mathcal{M}(i)=i} \cdot \eta, \forall i \in \{1, 2, \dots, C\}$.

2.2. Background

We consider sample selection methods (Jiang et al., 2018; Li et al., 2020) as the base of our approach, which has recently shown great promise in dealing with label noise. Typically, these methods divide training samples into the clean and noisy sets, denoted by \mathcal{X} and \mathcal{U} respectively. The labels of the clean set \mathcal{X} are used for supervised training, since it has a higher label precision, while the noisy set \mathcal{U} is treated unsupervised or simply abandoned due to its large noise ratio. A two-network structure is also commonly applied in state-of-the-art noise-robust models (Li et al., 2020; Cordeiro et al., 2021), where the two classifiers $f_{\theta_1}, f_{\theta_2}$ share the same structure but have different groups of parameters θ_1, θ_2 . The training of f_{θ_1} and f_{θ_2} is performed in a *co-teaching* manner (Han et al., 2018) (*i.e.*, the division made by a network is used by the other), to mutually reduce prediction error and achieve a favorable ensemble effect.

Another important factor is how to precisely pick out clean samples. A dynamic selection approach is based on loss modeling, namely the small-loss strategy, leveraging the fact that DNNs tend to learn simple patterns first before overfitting to noisy labels (Arpit et al., 2017). In (Arazo et al., 2019) and (Li et al., 2020), a clean probability is modeled for each sample as $P_i^{clean}(\ell_i, \{\ell_j\}_{j=1}^N, \gamma)$, with $\ell_i = -\sum_c \tilde{y}_i^c \cdot \log(f_{\theta}^c(\mathbf{x}_i))$ being the classification loss for sample i and γ being the hyper-parameter.

In this work, we fit a two-component Gaussian Mixture Model (GMM) (Permuter et al., 2006) to the loss distribution as in (Li et al., 2020), and P^{clean} is the posterior probability of the lower-mean component that fits small losses. In this

way, we can write the clean and noisy set as

$$\begin{aligned} \mathcal{X} &= \{(\mathbf{x}_i, \tilde{\mathbf{y}}_i) | (\mathbf{x}_i, \tilde{\mathbf{y}}_i) \in \mathcal{S}, P_i^{clean} \geq \tau_c\}, \\ \mathcal{U} &= \{(\mathbf{x}_i, p_i) | \mathbf{x}_i \in \mathcal{S}_{\mathbf{x}}, P_i^{clean} < \tau_c\}, \end{aligned} \quad (1)$$

where τ_c is the probability threshold for the clean set and $p_i = \frac{1}{2}(f_{\theta_1}(\mathbf{x}_i) + f_{\theta_2}(\mathbf{x}_i))$ is the softmax probabilities predicted jointly by f_{θ_1} and f_{θ_2} (Li et al., 2020).

After the division, the two classifiers $f_{\theta_1}, f_{\theta_2}$ are trained on \mathcal{X} and \mathcal{U} with a semi-supervised approach. Following (Li et al., 2020), we use MixMatch (Berthelot et al., 2019) to transform \mathcal{X} and \mathcal{U} into mixed clean and noisy sets \mathcal{X}' and \mathcal{U}' , where

$$\begin{aligned} \mathcal{X}' &= \{(l(\mathbf{x}_i, \mathbf{x}_j, \lambda), l(\tilde{\mathbf{y}}_i, \mathbf{y}_j, \lambda)) | \\ &\quad (\mathbf{x}_i, \tilde{\mathbf{y}}_i) \in \mathcal{X}, (\mathbf{x}_j, \mathbf{y}_j) \in \mathcal{X} \cup \mathcal{U}\}, \\ \mathcal{U}' &= \{(l(\mathbf{x}_i, \mathbf{x}_j, \lambda), l(p_i, \mathbf{y}_j, \lambda)) | \\ &\quad (\mathbf{x}_i, p_i) \in \mathcal{U}, (\mathbf{x}_j, \mathbf{y}_j) \in \mathcal{X} \cup \mathcal{U}\}, \end{aligned} \quad (2)$$

$l(\cdot, \cdot, \lambda)$ is the linear interpolation function (*e.g.*, $l(\mathbf{x}_i, \mathbf{x}_j, \lambda) = \lambda \mathbf{x}_i + (1 - \lambda) \mathbf{x}_j$), and $\lambda \sim \text{Beta}(\alpha, \alpha)$ is a real number within $[0, 1]$ sampled from a beta distribution. We make sure that $|\mathcal{X}| = |\mathcal{X}'|$ and $|\mathcal{U}| = |\mathcal{U}'|$. The training objective is to minimize

$$\mathcal{L}_{VR}(\mathcal{X}', \mathcal{U}') = \mathcal{L}_x(\mathcal{X}') + \lambda_u \mathcal{L}_u(\mathcal{U}') \quad (3)$$

with

$$\mathcal{L}_x(\mathcal{X}') = \frac{-1}{|\mathcal{X}'|} \sum_{\substack{(\mathbf{x}_i, \mathbf{y}_i') \\ \in \mathcal{X}'}} \sum_c \mathbf{y}_i'^c \cdot \log(f_{\theta}^c(\mathbf{x}_i)), \quad (4)$$

$$\mathcal{L}_u(\mathcal{U}') = \frac{1}{|\mathcal{U}'|} \sum_{\substack{(\mathbf{x}_i, \mathbf{y}_i') \\ \in \mathcal{U}'}} \|\mathbf{y}_i' - f_{\theta}(\mathbf{x}_i)\|_2^2, \quad (5)$$

where λ_u controls the strength of the unsupervised loss. This objective is known as vicinal risk minimization (VRM), which is shown to be capable of reducing the memorization of corrupt labels (Zhang et al., 2017b).

3. Methodology

3.1. Overview of the LC-Booster

An overview of the LC-Booster framework is presented in Fig. 2. We first warm up the model for a few iterations by training with all data, so that some easy patterns can be learned first. Then, we divide samples into clean and noisy sets \mathcal{X}, \mathcal{U} defined in Eq. 1, and use MixMatch (Berthelot et al., 2019) to train the model. For better generalization, we adopt a hybrid augmentation (H-Aug.) strategy that transforms images into weak and strong augmented views. We directly utilize the labels to calculate the Cross-Entropy

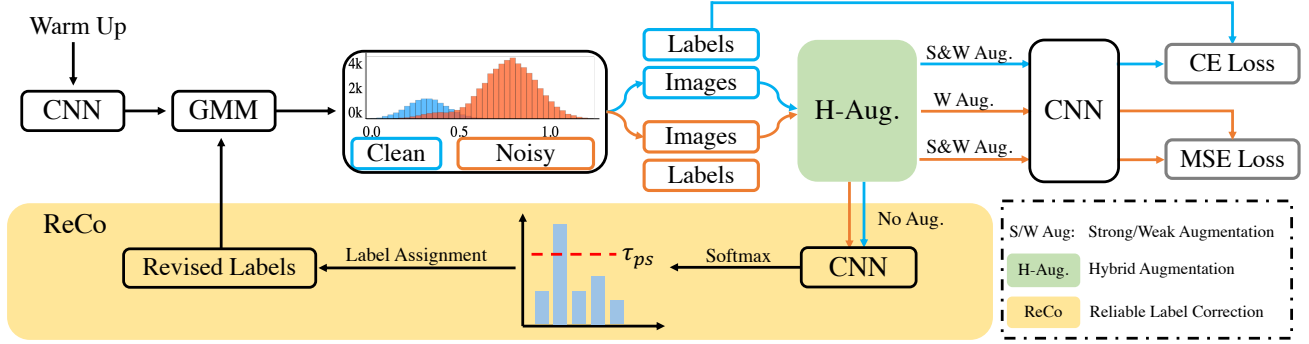


Figure 2. An overview of the proposed LC-Booster framework. We first warm up the model for a few iterations, and then fit a GMM to the loss distribution to separate clean or noisy sets. We then adopt H-Aug, which enforces consistency between weak-weak and weak-strong views. During training, we perform ReCo to revise the labels for all samples. The revised labels are used for GMM and CE Loss in the following epochs.

Loss (CE Loss) for clean samples and minimize the Mean Square Error Loss (MSE Loss) between weak-weak and weak-strong views of noisy samples. At around the middle stage, Reliable Label Correction (ReCo) is adopted to revise the labels in both clean and noisy sets. The revised labels are used in the rest of the training, where a larger clean set could be selected based on GMM loss modeling.

3.2. Reliable Label Correction

Reliable Label Correction (ReCo) aims to deal with the meagre clean set problem in sample selection methods. With such a small labeled clean set, the generalization performance of a network could degenerate significantly, since DNNs are known to be data-hungry. To better leverage the noisy data, we propose to revise the labels in the training set \mathcal{S} based on network predictions, so that more samples could be involved in the clean set with supervised signals. Specifically, we perform label correction by assigning those high confidence samples with hard pseudo labels, which are in accordance with their highest predictions. This gives us a new training set $\hat{\mathcal{S}}$ that mixes both raw and pseudo labels. Formally, it can be written as

$$\begin{aligned}\hat{\mathcal{S}}_r &= \{(\mathbf{x}_i, \tilde{\mathbf{y}}_i) | \forall (\mathbf{x}_i, \tilde{\mathbf{y}}_i) \in \mathcal{S} : \max_c p_i^c < \tau_{ps}\}, \\ \hat{\mathcal{S}}_{ps} &= \{(\mathbf{x}_i, e^k) | \forall \mathbf{x}_i \in \mathcal{S}_x : \max_c p_i^c \geq \tau_{ps}, k = \arg\max_c p_i^c\}, \\ \hat{\mathcal{S}} &= \hat{\mathcal{S}}_r \cup \hat{\mathcal{S}}_{ps},\end{aligned}\quad (6)$$

where $p_i = \frac{1}{2}(f_{\theta_1}(\mathbf{x}_i) + f_{\theta_2}(\mathbf{x}_i))$ is the softmax probability jointly predicted by f_{θ_1} and f_{θ_2} , and τ_{ps} is the confidence threshold for label correction. The average predictions of the two networks could alleviate the confirmation bias of self-training, and achieve a favorable ensemble effect. Furthermore, the precision of revised labels can be guaranteed with a proper choice of τ_{ps} , as shown in the following Theorem 1.

Theorem 1. (Yang et al., 2021) Assume $\tilde{\alpha}_c(\mathbf{x})$ denotes the conditional probability $P_{\mathcal{D}_X, \mathcal{D}_Y}(\tilde{Y} = e_c | X = \mathbf{x})$, and $\alpha_c(\mathbf{x}) = P_{\mathcal{D}_X, \mathcal{D}_Y}(Y = e_c | X = \mathbf{x})$. $\forall \mathbf{x} \sim \mathcal{D}_X$, we have

$$\tilde{\alpha}_c(\mathbf{x}) > \frac{1 + \rho_c}{2} \implies \alpha_c(\mathbf{x}) > \frac{1}{2}. \quad (7)$$

Theorem 1 provides us with the guidance of choosing proper τ_{ps} for label correction. By setting $\tau_{ps} = \frac{1+\rho_c}{2}$, we can ensure that the index of the highest prediction is the true class for sample \mathbf{x} , as no other class has a higher probability than $\alpha_c(\mathbf{x})$. In practice, however, ρ_c in Eq. 7 is usually an unknown value, which needs to be estimated. We discuss the problem and study the choice of ReCo hyper-parameters in Sec. 4.3. The proof of Theorem 1 is provided in Appendix A.

3.3. Hybrid Augmentation

Inspired by (Sohn et al., 2020), we seek to enhance the model’s generalization and discrimination ability by applying strong augmentation. However, in the proposed framework, the augmentation policy needs to be carefully designed to avoid adversely affecting sample selection or label correction. To this end, we adopt a hybrid weak-strong augmentation strategy for accurate prediction, efficient training, and improving generalization and discrimination. In our experiments, weak augmentation involves flipping and random cropping, and strong augmentation refers to AutoAugment (Cubuk et al., 2018) or RandAugment (Cubuk et al., 2020) based on different datasets and different noise rates.

In the process of loss modeling and label correction, we simply use raw images (or center crops) for inference and abandon any spatial or color distortion. The goal is to obtain accurate modeling of loss distribution/class probabilities for the best sample selection/label correction. Following (Sohn

et al., 2020) and (Nishi et al., 2021), we apply weak augmentation when performing pseudo labeling on the noisy set \mathcal{U} in Eq. 1. The pseudo label is then used by its source image as well as another strong augmented view for optimizing the two networks f_{θ_1} and f_{θ_2} . As a result, consistency is enforced on both weak-weak and weak-strong views. This is different from (Nishi et al., 2021) where the batches for pseudo labeling and optimization are different and disjoint. Our hybrid augmentation strategy could save memory and computation costs while improving generalization with hybrid consistency regularization.

3.4. Training Objective

We denote the divided clean and noisy sets after label correction as

$$\begin{aligned}\hat{\mathcal{X}} &= \{(\mathbf{x}_i, \hat{\mathbf{y}}_i) | (\mathbf{x}_i, \hat{\mathbf{y}}_i) \in \hat{\mathcal{S}}, P_i^{clean} \geq \tau_c\}, \\ \hat{\mathcal{U}} &= \{(\mathbf{x}_i, p_i) | \mathbf{x}_i \in \hat{\mathcal{S}}, P_i^{clean} < \tau_c\},\end{aligned}\quad (8)$$

and the correspondent mixed sets as

$$\begin{aligned}\hat{\mathcal{X}}' &= \{(l(\mathbf{x}_i, \mathbf{x}_j, \lambda), l(\hat{\mathbf{y}}_i, \mathbf{y}_j, \lambda)) | \\ &\quad (\mathbf{x}_i, \hat{\mathbf{y}}_i) \in \hat{\mathcal{X}}, (\mathbf{x}_j, \mathbf{y}_j) \in \hat{\mathcal{X}} \cup \hat{\mathcal{U}}\}, \\ \hat{\mathcal{U}}' &= \{(l(\mathbf{x}_i, \mathbf{x}_j, \lambda), l(p_i, \mathbf{y}_j, \lambda)) | \\ &\quad (\mathbf{x}_i, p_i) \in \hat{\mathcal{U}}, (\mathbf{x}_j, \mathbf{y}_j) \in \hat{\mathcal{X}} \cup \hat{\mathcal{U}}\}.\end{aligned}\quad (9)$$

The final training loss of LC-Booster is

$$\mathcal{L} = \begin{cases} \mathcal{L}_{VR}(\mathcal{X}', \mathcal{U}') + \lambda_r \mathcal{L}_{reg}, & \text{before ReCo,} \\ \mathcal{L}_{VR}(\hat{\mathcal{X}}', \hat{\mathcal{U}}') + \lambda_r \mathcal{L}_{reg}, & \text{after ReCo,} \end{cases}\quad (10)$$

where \mathcal{L}_{VR} is defined in Eq. 3, λ_r is the weight of regularization and

$$\mathcal{L}_{reg} = \sum_c \pi_c \log \left(\pi_c / \frac{\sum_{\mathbf{x}_i \in \mathcal{X}' \cup \mathcal{U}'} f_{\theta}^c(\mathbf{x}_i)}{|\mathcal{X}'| + |\mathcal{U}'|} \right). \quad (11)$$

We apply the same regularization term \mathcal{L}_{reg} as in (Tanaka et al., 2018; Li et al., 2020). The intuition is that it uses a uniform distribution π (i.e., $\pi_c = \frac{1}{C}$) to encourage the average output of all samples to be equal for each class.

4. Experiments

In this section, we conduct comprehensive experiments to evaluate the proposed LC-Booster. We first introduce the datasets and implementation details in Sec. 4.1. Then, we compare LC-Booster with state-of-the-art methods on CIFAR-10/100, Clothing1M, and WebVision in Sec. 4.2. In Sec. 4.3, we provide extensive ablation studies to illustrate the effects of our method. Last, in Sec. 4.4, qualitative visualization results are presented to demonstrate the superiority of LC-Booster.

4.1. Datasets and Implementation Details

We extensively validate the effectiveness of LC-Booster on four noisy-label benchmarks, namely CIFAR-10, CIFAR-100 (Krizhevsky et al., 2009), Clothing1M (Xiao et al., 2015) and WebVision (Li et al., 2017). CIFAR-10 and CIFAR-100 contain 60K images of size 32×32 , with 50K for training and 10K for testing. Clothing1M and WebVision are two large-scale datasets with real-world noisy labels. Clothing1M consists of 1 million training images crawled from online shopping websites and is composed of 14 classes. Labels of Clothing1M are generated from surrounding texts and the overall noise ratio is estimated to be around 40%. WebVision contains 2.4 million images collected from the Internet, with the same 1000 classes as in ILSVRC12 (Deng et al., 2009). Following previous works (Chen et al., 2019; Li et al., 2020), we only use the first 50 classes of the Google image subset for training and test.

For CIFAR-10/100, we experiment with symmetric and asymmetric label noise \tilde{Y}_{sym} and \tilde{Y}_{asym} as described in Sec. 2.1, following the protocol in previous works (Li et al., 2019a; 2020; Nishi et al., 2021). We use an 18-layer PreAct ResNet (PRN18) (He et al., 2016) as the network backbone and train it for roughly 300 epochs, following (Nishi et al., 2021). We adopt SGD as the optimizer with a batch size of 64, a momentum of 0.9, and a weight decay of 0.0005. The initial learning rate is 0.02 and is decayed by a factor of 10 in the middle of training. The warm up period is 10 epochs for CIFAR-10 and 30 epochs for CIFAR-100. As for our method, we perform ReCo at the 100th epoch and set different τ_{ps} for different noise rates (see Appendix B). A discussion is also provided in Sec. 4.3 about the choice of the two hyper-parameters.

Following previous baseline methods (Li et al., 2020; Cordeiro et al., 2021), we use ImageNet pre-trained ResNet-50 as the backbone for Clothing1M, and use Inception-ResNet v2 (Szegedy et al., 2017) as the backbone for WebVision. More training details and hyper-parameters of the two datasets are delineated in Appendix B.

4.2. Comparison with State-of-the-art Methods

We compare LC-Booster with recent state-of-the-art methods, including Mixup (Zhang et al., 2017b), M-correction (Arazo et al., 2019), Meta-Learning (Li et al., 2019b), ELR⁺ (Liu et al., 2020), DivideMix (Li et al., 2020), LongReMix (Cordeiro et al., 2021), DM-AugDesc (Nishi et al., 2021). We also compare it with previous label correction methods Bootstrapping (Reed et al., 2014) and MSLC (Wu et al., 2020). For a fair comparison, we adopt the same backbone as in previous works for all benchmarks.

Dataset		CIFAR-10					CIFAR-100				
Noise type		Sym.					Asym.				
Methods\Noise ratio		20%	50%	80%	90%	40%	20%	50%	80%	90%	
Cross-Entropy	Best	86.8	79.4	62.9	42.7	85.0	62.0	46.7	19.9	10.1	
	Last	82.7	57.9	26.1	16.8	72.3	61.8	37.3	8.8	3.5	
Mixup (Zhang et al., 2017b)	Best	85.6	87.1	71.6	52.2	-	67.8	57.3	30.8	14.6	
	Last	92.3	77.3	46.7	43.9	-	66.0	46.6	17.6	8.1	
Bootstrapping (Reed et al., 2014)	Best	91.5	-	63.8	-	91.2	69.8	-	17.6	-	
	Last	88.0	-	63.4	-	85.6	63.0	-	17.0	-	
MSLC (Wu et al., 2020)	Best	93.5	-	69.9	-	92.8	72.5	-	24.3	-	
	Last	93.4	-	68.9	-	92.5	72.0	-	20.5	-	
M-correction (Arazo et al., 2019)	Best	94.0	92.0	86.8	69.1	87.4	73.9	66.1	48.2	24.3	
	Last	93.8	91.9	86.6	68.7	86.3	73.4	65.4	47.6	20.5	
Meta-Learning (Li et al., 2019b)	Best	92.9	89.3	77.4	58.7	89.2	68.5	59.2	42.4	19.5	
	Last	92.0	88.8	76.1	58.3	88.6	67.7	58.0	40.1	14.3	
ELR ⁺ (Liu et al., 2020)	Best	95.8	94.8	93.3	78.7	93.0	77.6	73.6	60.8	33.4	
	Last	-	-	-	-	-	-	-	-	-	
DivideMix (Li et al., 2020)	Best	96.1	94.6	93.2	76.0	93.4	77.3	74.6	60.2	31.5	
	Last	95.7	94.4	92.9	75.4	92.1	76.9	74.2	59.6	31.0	
LongReMix (Cordeiro et al., 2021)	Best	96.2	95.0	93.9	82.0	94.7	77.8	75.6	62.9	33.8	
	Last	96.0	94.7	93.4	81.3	94.3	77.5	75.1	62.3	33.2	
DM-AugDesc-WS-WAW (Nishi et al., 2021)	Best	96.3	95.4	93.8	91.9	94.6	79.5	77.2	66.4	41.2	
	Last	96.2	95.1	93.6	91.8	94.3	79.2	77.0	66.1	40.9	
LC-Booster	Best	96.4	95.6	94.7	93.5	95.1	79.6	77.6	66.9	48.4	
	Last	96.3	95.3	94.4	93.1	95.0	79.5	77.4	66.5	48.1	

Table 1. Comparison with state-of-the-art methods on CIFAR-10 and CIFAR-100 with symmetric (from 20% to 90%) and asymmetric noise (40%). We report both the best test accuracy across all epochs and the averaged test accuracy over the last 10 epochs of training. Results of previous methods are cited from their original papers. **Bold entries** are best results.

Method	Test Accuracy
Cross-Entropy	69.21
F-correction (Patrini et al., 2017)	69.84
M-correction (Arazo et al., 2019)	71.00
Joint-Optim (Tanaka et al., 2018)	72.16
Meta-Cleaner (Zhang et al., 2019)	72.50
Meta-Learning (Li et al., 2019b)	73.47
P-correction (Yi & Wu, 2019)	73.49
AFM (Peng et al., 2020)	74.12
SMP (Han et al., 2019)	74.45
DivideMix (Li et al., 2020)	74.76
ELR+ (Liu et al., 2020)	74.81
LongReMix (Cordeiro et al., 2021)	74.38
DM-AugDesc (Nishi et al., 2021)	75.11
Ours	75.23

Table 2. Comparison with state-of-the-art methods in test accuracy (%) on Clothing1M. Results for baseline methods are cited from original papers. The best entry is marked in **bold**.

Comparison of synthetic noisy labels. The results of CIFAR-10/100 are present in Tab.1. We experiment with different levels of symmetric label noise ranging from 20%

to 90%, as well as 40% asymmetric noise for CIFAR-10. Following the metrics in previous works, we report both the best test accuracy across all epochs and the average test accuracy over the last 10 epochs of training. Our LC-Booster outperforms previous state-of-the-art methods across all noise ratios. A remarkable improvement can be seen under the 90% high noise rate, where 1.6% and 7.2% absolute accuracy gains are achieved on CIFAR-10 and CIFAR-100 respectively. This demonstrates the robustness of our method against extreme label noise. Moreover, our method also outperforms previous label correction methods (Bootstrapping, MSLC) by a large margin, which verifies our idea that label correction could be better leveraged with sample selection.

Comparison of real-world noisy labels. We also validate our method on large-scale noisy labeled data sets. Tab. 2 evaluates LC-Booster on Clothing1M. Our method outperforms previous methods by at least 0.12% absolute test accuracy. Tab. 3 shows the validation results on (mini) WebVision and ILSVRC12. LC-Booster achieves comparable results on WebVision and state-of-the-art performance on ILSVRC12. These results show that our method can be

well applied in real-world scenarios with large-scale data.

Method	WebVision		ILSVRC12	
	Top1	Top5	Top1	Top5
F-correction (Patrini et al., 2017)	61.12	82.68	57.36	82.36
Decoupling (Malach, 2017)	62.54	84.74	58.26	82.26
D2L (Ma et al., 2018)	62.68	84.00	57.80	81.36
MentorNet (Jiang et al., 2018)	63.00	81.40	57.80	79.92
Co-teaching (Han et al., 2018)	63.58	85.20	61.48	84.70
Iterative-CV (Chen et al., 2019)	65.24	85.34	61.60	84.98
DivideMix (Li et al., 2020)	77.32	91.64	75.20	90.84
LongReMix (Cordeiro et al., 2021)	78.92	92.32	-	-
NGC (Wu et al., 2021)	79.16	91.84	74.44	91.04
Ours	78.29	92.18	75.44	91.26

Table 3. Comparison with state-of-the-art methods trained on (mini) WebVision dataset. Numbers denote top-1 (top-5) accuracy (%) on the WebVision validation set and the ILSVRC12 validation set. Results for baseline methods are cited from their original papers. **Bold entries** are best results.

4.3. Ablation Studies

We perform extensive ablation studies to illustrate the effects of our method. For better evaluation, we conduct experiments on CIFAR-10 with 90% symmetric noise and report the best test accuracy (if not otherwise stated).

Evaluation of ReCo and H-Aug. We first analyze the effect of the two modules of LC-Booster: H-Aug. and ReCo. Experimental results are shown in Tab. 4. As one can see, the best results are achieved when ReCo and H-Aug. are jointly used, which shows the compatibility of the two modules. Applying either of the two modules individually also brings non-trivial accuracy gain. Moreover, we find that applying ReCo with H-Aug. could obtain a larger improvement than applying ReCo alone (3.7% vs. 1.4% on CIFAR-10, 6.6% vs. 4.8% on CIFAR-100), which indicates that the advantage of ReCo could be better exploited with a proper augmentation strategy.

ReCo	H-Aug.	CIFAR-10	CIFAR-100
		83.9	31.5
✓		85.3	36.3
	✓	89.8	41.8
✓	✓	93.5	48.4

Table 4. Evaluation of ReCo and H-Aug. in the proposed framework. The noise type is 90% symmetric noise for both CIFAR-10 and CIFAR-100. **Bold entries** are best results.

Exploring τ_{ps} . τ_{ps} is defined in Eq. 6 as the threshold for ReCo. It is proved in Theorem 1 that setting $\tau_{ps} = \frac{1+\rho_c}{2}$ guarantees the revised labels are correct. In practice, however, a problem remains that ρ_c needs to be estimated given a noisy dataset. Specifically, in the proposed framework, ρ_c is still hard to estimate even if the overall noise ratio is

determined beforehand (e.g., 90% symmetric noise). This is because the noise distribution of the clean/noisy set is still unknown and probably changing during training. As this, we simply use $\frac{1+\rho_c}{2}$ as the *upper bound* of τ_{ps} , and fine-tune τ_{ps} from that point for best performance. We present the test accuracy for different τ_{ps} in Tab. 5, as well as the number of revised samples $|\hat{\mathcal{S}}_{ps}|$ and label precision of $\hat{\mathcal{S}}_{ps}$ for better illustration. One can find that $|\hat{\mathcal{S}}_{ps}|$ decreases monotonically as τ_{ps} rises. At the same time, the label precision increases and finally arrives at 100% when τ_{ps} grows up to 0.95, which is in accordance with Theorem 1 when $\rho_c = 0.9$. However, even if $\hat{\mathcal{S}}_{ps}$ is absolutely clean when $\tau_{ps} = 0.95$, $|\hat{\mathcal{S}}_{ps}|$ significantly shrinks to less than 500, which is only 1% of total training data. Such a small $\hat{\mathcal{S}}_{ps}$ can make little change to the total number of clean training samples and could hardly boost model performance. Hence, we discreetly sacrifice the label precision by decreasing τ_{ps} , in exchange for a larger $\hat{\mathcal{S}}_{ps}$. With this sacrifice, a more favorable balance could be achieved between the purity and quantity of revised samples, as shown in Tab. 5 that the best accuracy is achieved when $\tau_{ps} = 0.8$. Further decreasing τ_{ps} leads to inferior performance, as more wrongly predicted labels are imbued into $\hat{\mathcal{S}}_{ps}$. More details are available in Appendix B.

τ_{ps}	0.0	0.5	0.7	0.8	0.95
$ \hat{\mathcal{S}}_{ps} $	50000	42641	29715	13405	483
Label Pres. (%)	84.6	91.5	97.4	99.1	100.0
Test Acc. (%)	84.9	90.5	93.4	93.5	91.3

Table 5. Exploration of different τ_{ps} . $\hat{\mathcal{S}}_{ps}$ is defined in Eq. 6 as the set of revised samples. Label Pres. denotes the label precision of $\hat{\mathcal{S}}_{ps}$. The last row is test accuracy on CIFAR-10 with 90% symmetric noise. The best result is marked in **bold**.

Exploring when to perform ReCo. Here, we investigate when to perform ReCo, the other hyper-parameter of the proposed method. We study its effect by varying the re-labeling epoch from 50 to 250, with a total of 300 training epochs and $\tau_{ps} = 0.8$ as discussed above. As shown in Tab. 6, the best performance of 93.5% is achieved at the 100th epoch, which is before the right middle of training. After that, the test accuracy begins to drop. We hypothesize that this is because the model gradually overfits to noisy samples as training progresses, making the predictions less reliable. We also try to perform ReCo multiple times (last column of Tab. 6, at both 100th and 200th epoch). However, this does not bring further accuracy gain, which indicates that re-labeling once is sufficient.

Comparison on re-training performance. Here, we compare the re-labeling quality of LC-Booster with other methods. We first re-label the noisy dataset with the trained model. Then, a randomly initialized PRN18 is trained from

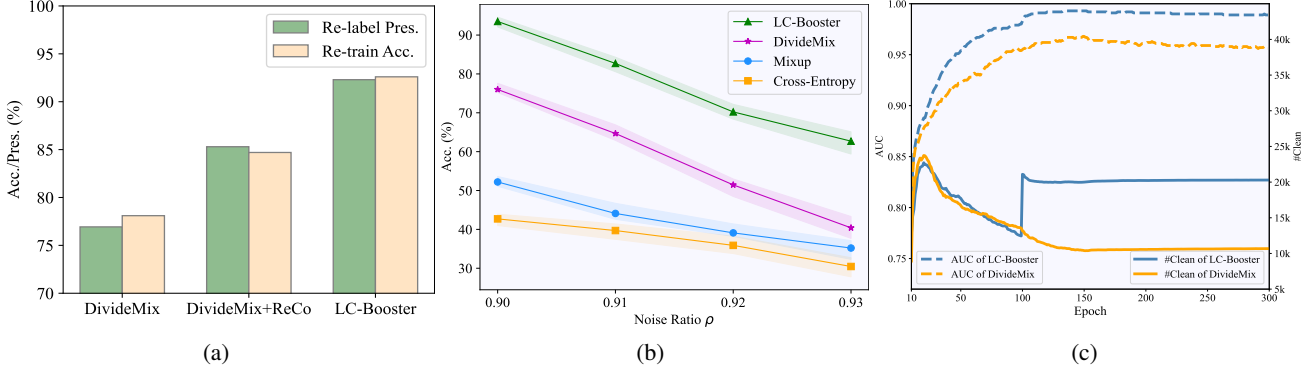


Figure 3. (a) compares the precision of re-labeling (Re-label Pres.) and re-training accuracy (Re-train Acc.) between different methods. Higher indicates stronger cleansing ability. (b) shows the results under even higher extreme label noises, *i.e.*, $\geq 90\%$. (c) shows the curves of AUC and size of the clean set (#Clean) on CIFAR-10 with 90% symmetric noise. Higher AUC indicates that clean samples are selected more precisely based on GMM.

Epoch(s)	50	100	150	200	250	100&200
Test Acc. (%)	91.9	93.5	91.5	90.3	89.7	93.3

Table 6. Exploring which epoch(s) to perform ReCo. The last column means re-labeling twice at the 100th and 200th epoch. The best result is marked in **bold**.

scratch using re-labeled samples. We compare both the precision of new labels and test accuracy of re-trained models in Fig. 3(a). It can be seen in the figure that our method achieves the highest re-labeling precision and re-training accuracy. Remarkably, the re-labeling precision achieves over 90% under 90% symmetric noise, demonstrating the superior cleansing ability of our method. Moreover, simply applying ReCo with DivideMix could also obtain a higher re-labeling precision as well as re-training accuracy.

Evaluation under extreme label noises. We evaluate the robustness of our method under even higher extreme label noises, *i.e.*, $\geq 90\%$ symmetric noise. To the best of our knowledge, no previous attempts have been made under such heavy label noise. The results are shown in Fig. 3(b). LC-Booster consistently achieves the best results across all noise rates. Furthermore, it can also be observed that the performance gap between LC-Booster and DivideMix increases as the noise rate grows from 90% to 93%. This demonstrates the superior robustness of our method under extreme label noise.

4.4. Visualization

Learned embeddings. We compare the distributions of embedded features of DivideMix and our LC-Booster using t-SNE in Fig. 4. For explicitness, we only visualize the first three classes of CIFAR-10 with 90% symmetric noise. A complete distribution of 10 classes is provided

in Appendix C. One can see that there exist some obvious outliers of DivideMix, while features of our method are better clustered. Moreover, LC-Booster has fewer false predictions (marked as triangles) compared with DivideMix, demonstrating its robustness under a high noise ratio.

AUC and size of clean set. We show the dynamics of AUC and the size of the clean set in Fig. 3(c). Numbers are from experiments on CIFAR-10 with 90% symmetric noise. We use the clean probabilities output by GMM for calculating AUC. As shown in the figure, LC-Booster consistently achieves higher AUC than DivideMix during training, which shows that our method is able to select clean samples more precisely. Moreover, after the 100th epoch of performing ReCo, the size of the clean set in LC-Booster significantly rises and surpasses that of DivideMix by a large margin. The effective expansion of the clean set helps to explain the superior performance of our method. More curves of performing ReCo at different epochs are shown in Appendix C.

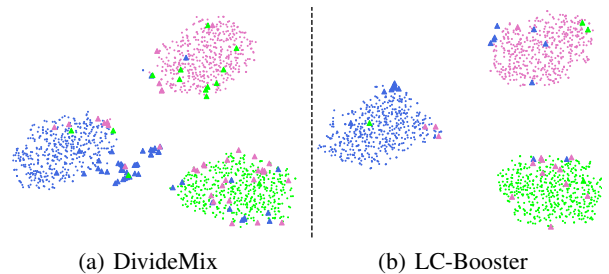


Figure 4. Visualization of embedded features on CIFAR-10 with 90% symmetric noise. Three colors indicate the first three classes of CIFAR-10. Correct predictions are marked as circles and false predictions as triangles. Best viewed in color.

5. Conclusion

In this paper, we propose LC-Booster, a novel framework for learning with extremely noisy labels. LC-Booster naturally

leverages label correction with sample selection, to make a larger and more purified clean set that effectively boosts model performance. Through extensive experiments on multiple benchmarks, we show that LC-Booster consistently demonstrates superior performance compared with state-of-the-art methods. We hope the proposed learning paradigm could inspire future research along this direction for the problem of LNL.

Acknowledge. This research is supported by the National Research Foundation, Singapore under its AI Singapore Programme (AISG Award No: AISG2-PhD-2021-08-008), NUS Faculty Research Committee Grant (WBS: A-0009440-00-00), and the EPSRC programme grant Visual AI EP/T028572/1. We thank Google TFRC for supporting us to get access to the Cloud TPUs. We thank CSCS (Swiss National Supercomputing Centre) for supporting us to get access to the Piz Daint supercomputer. We thank TACC (Texas Advanced Computing Center) for supporting us to get access to the Longhorn supercomputer and the Frontera supercomputer. We thank LuxProvide (Luxembourg national supercomputer HPC organization) for supporting us to get access to the MeluXina supercomputer.

References

- Allen-Zhu, Z., Li, Y., and Liang, Y. Learning and generalization in overparameterized neural networks, going beyond two layers. *arXiv preprint arXiv:1811.04918*, 2018.
- Arazo, E., Ortego, D., Albert, P., O’Connor, N., and McGuinness, K. Unsupervised label noise modeling and loss correction. In *ICML*, pp. 312–321, 2019.
- Arazo, E., Ortego, D., Albert, P., O’Connor, N. E., and McGuinness, K. Pseudo-labeling and confirmation bias in deep semi-supervised learning. In *IJCNN*, pp. 1–8, 2020.
- Arpit, D., Jastrzebski, S., Ballas, N., Krueger, D., Bengio, E., Kanwal, M. S., Maharaj, T., Fischer, A., Courville, A., Bengio, Y., et al. A closer look at memorization in deep networks. In *ICML*, pp. 233–242, 2017.
- Berthelot, D., Carlini, N., Goodfellow, I., Papernot, N., Oliver, A., and Raffel, C. Mixmatch: A holistic approach to semi-supervised learning. *arXiv preprint arXiv:1905.02249*, 2019.
- Chen, P., Liao, B. B., Chen, G., and Zhang, S. Understanding and utilizing deep neural networks trained with noisy labels. In *ICML*, pp. 1062–1070, 2019.
- Cordeiro, F. R., Sachdeva, R., Belagiannis, V., Reid, I., and Carneiro, G. Longremix: Robust learning with high confidence samples in a noisy label environment. *arXiv preprint arXiv:2103.04173*, 2021.
- Cubuk, E. D., Zoph, B., Mane, D., Vasudevan, V., and Le, Q. V. Autoaugment: Learning augmentation policies from data. *arXiv preprint arXiv:1805.09501*, 2018.
- Cubuk, E. D., Zoph, B., Shlens, J., and Le, Q. V. Randaugument: Practical automated data augmentation with a reduced search space. In *CVPR Workshops*, pp. 702–703, 2020.
- Deng, J., Dong, W., Socher, R., Li, L.-J., Li, K., and Fei-Fei, L. Imagenet: A large-scale hierarchical image database. In *CVPR*, pp. 248–255, 2009.
- Frénay, B. and Verleysen, M. Classification in the presence of label noise: a survey. *IEEE TNNLS*, 25(5):845–869, 2013.
- Han, B., Yao, Q., Yu, X., Niu, G., Xu, M., Hu, W., Tsang, I., and Sugiyama, M. Co-teaching: Robust training of deep neural networks with extremely noisy labels. *arXiv preprint arXiv:1804.06872*, 2018.
- Han, J., Luo, P., and Wang, X. Deep self-learning from noisy labels. In *ICCV*, pp. 5138–5147, 2019.
- He, K., Zhang, X., Ren, S., and Sun, J. Identity mappings in deep residual networks. In *ECCV*, pp. 630–645, 2016.
- Jiang, L., Zhou, Z., Leung, T., Li, L.-J., and Fei-Fei, L. Mentornet: Learning data-driven curriculum for very deep neural networks on corrupted labels. In *ICML*, pp. 2304–2313, 2018.
- Krizhevsky, A., Hinton, G., et al. Learning multiple layers of features from tiny images. 2009.
- Kuznetsova, A., Rom, H., Alldrin, N., Uijlings, J., Krasin, I., Pont-Tuset, J., Kamali, S., Popov, S., Mallocci, M., Kolesnikov, A., et al. The open images dataset v4. *IJCV*, 128(7):1956–1981, 2020.
- Li, J., Wong, Y., Zhao, Q., and Kankanhalli, M. S. Learning to learn from noisy labeled data. In *CVPR*, June 2019a.
- Li, J., Wong, Y., Zhao, Q., and Kankanhalli, M. S. Learning to learn from noisy labeled data. In *CVPR*, pp. 5051–5059, 2019b.
- Li, J., Socher, R., and Hoi, S. C. Dividemix: Learning with noisy labels as semi-supervised learning. *arXiv preprint arXiv:2002.07394*, 2020.
- Li, W., Wang, L., Li, W., Agustsson, E., and Van Gool, L. Webvision database: Visual learning and understanding from web data. *arXiv preprint arXiv:1708.02862*, 2017.

- Liu, S., Niles-Weed, J., Razavian, N., and Fernandez-Granda, C. Early-learning regularization prevents memorization of noisy labels. *arXiv preprint arXiv:2007.00151*, 2020.
- Ma, X., Wang, Y., Houle, M. E., Zhou, S., Erfani, S., Xia, S., Wijewickrema, S., and Bailey, J. Dimensionality-driven learning with noisy labels. In *ICML*, pp. 3355–3364, 2018.
- Mahajan, D., Girshick, R., Ramanathan, V., He, K., Paluri, M., Li, Y., Bharambe, A., and Van Der Maaten, L. Exploring the limits of weakly supervised pretraining. In *ECCV*, pp. 181–196, 2018.
- Malach, Eran, S.-S. Decoupling” when to update” from” how to update”. *arXiv preprint arXiv:1706.02613*, 2017.
- Nishi, K., Ding, Y., Rich, A., and Hollerer, T. Augmentation strategies for learning with noisy labels. In *CVPR*, pp. 8022–8031, 2021.
- Patrini, G., Rozza, A., Krishna Menon, A., Nock, R., and Qu, L. Making deep neural networks robust to label noise: A loss correction approach. In *CVPR*, pp. 1944–1952, 2017.
- Peng, X., Wang, K., Zeng, Z., Li, Q., Yang, J., and Qiao, Y. Suppressing mislabeled data via grouping and self-attention. In *ECCV*, pp. 786–802, 2020.
- Permuter, H., Francos, J., and Jermyn, I. A study of gaussian mixture models of color and texture features for image classification and segmentation. *Pattern Recognition*, 39(4):695–706, 2006.
- Reed, S., Lee, H., Anguelov, D., Szegedy, C., Erhan, D., and Rabinovich, A. Training deep neural networks on noisy labels with bootstrapping. *arXiv preprint arXiv:1412.6596*, 2014.
- Sohn, K., Berthelot, D., Li, C.-L., Zhang, Z., Carlini, N., Cubuk, E. D., Kurakin, A., Zhang, H., and Raffel, C. Fix-match: Simplifying semi-supervised learning with consistency and confidence. *arXiv preprint arXiv:2001.07685*, 2020.
- Szegedy, C., Ioffe, S., Vanhoucke, V., and Alemi, A. A. Inception-v4, inception-resnet and the impact of residual connections on learning. In *AAAI*, 2017.
- Tanaka, D., Ikami, D., Yamasaki, T., and Aizawa, K. Joint optimization framework for learning with noisy labels. In *CVPR*, pp. 5552–5560, 2018.
- Wang, K., Peng, X., Yang, J., Lu, S., and Qiao, Y. Suppressing uncertainties for large-scale facial expression recognition. In *CVPR*, pp. 6897–6906, 2020.
- Wu, Y., Shu, J., Xie, Q., Zhao, Q., and Meng, D. Learning to purify noisy labels via meta soft label corrector. *arXiv preprint arXiv:2008.00627*, 2020.
- Wu, Z.-F., Wei, T., Jiang, J., Mao, C., Tang, M., and Li, Y.-F. Ngc: A unified framework for learning with open-world noisy data. In *ICCV*, pp. 62–71, 2021.
- Xiao, T., Xia, T., Yang, Y., Huang, C., and Wang, X. Learning from massive noisy labeled data for image classification. In *CVPR*, June 2015.
- Yang, S., Yang, E., Han, B., Liu, Y., Xu, M., Niu, G., and Liu, T. Estimating instance-dependent label-noise transition matrix using dnns. *arXiv preprint arXiv:2105.13001*, 2021.
- Yi, K. and Wu, J. Probabilistic end-to-end noise correction for learning with noisy labels. In *CVPR*, pp. 7017–7025, 2019.
- Yu, X., Han, B., Yao, J., Niu, G., Tsang, I., and Sugiyama, M. How does disagreement help generalization against label corruption? In *ICML*, pp. 7164–7173, 2019.
- Zhang, C., Bengio, S., Hardt, M., Recht, B., and Vinyals, O. Understanding deep learning requires rethinking generalization, 2017a.
- Zhang, H., Cisse, M., Dauphin, Y. N., and Lopez-Paz, D. mixup: Beyond empirical risk minimization. *arXiv preprint arXiv:1710.09412*, 2017b.
- Zhang, W., Wang, Y., and Qiao, Y. Metacleaner: Learning to hallucinate clean representations for noisy-labeled visual recognition. In *CVPR*, pp. 7373–7382, 2019.
- Zhang, Z., Zhang, H., Arik, S. O., Lee, H., and Pfister, T. Distilling effective supervision from severe label noise. In *CVPR*, pp. 9294–9303, 2020.

A. Proof of Theorem 1

Proof: $\forall \mathbf{x} \in \mathcal{X}$, $\tilde{\alpha}_c(\mathbf{x})$ can be rewritten as:

$$\begin{aligned}
 \tilde{\alpha}_c(\mathbf{x}) &= P(\tilde{Y} = e_c, Y = e_c \mid \mathbf{x}) + P(\tilde{Y} = e_c, Y \neq e_c \mid \mathbf{x}) \\
 &= P(\tilde{Y} = e_c \mid Y = e_c)P(Y = e_c \mid \mathbf{x}) \\
 &\quad + P(\tilde{Y} = e_c \mid Y \neq e_c)P(Y \neq e_c \mid \mathbf{x}) \\
 &= P(\tilde{Y} = e_c \mid Y = e_c)\alpha_c(\mathbf{x}) + \rho_c(1 - \alpha_c(\mathbf{x})) \\
 &\leq \alpha_c(\mathbf{x}) + \rho_c(1 - \alpha_c(\mathbf{x})) \\
 &= (1 - \rho_c)\alpha_c(\mathbf{x}) + \rho_c
 \end{aligned} \tag{12}$$

If $\alpha_c(\mathbf{x}) \leq \frac{1}{2}$, we have

$$\begin{aligned}
 \tilde{\alpha}_c(\mathbf{x}) &\leq (1 - \rho_c)\alpha_c(\mathbf{x}) + \rho_c \\
 &\leq \frac{1}{2}(1 - \rho_c) + \rho_c \\
 &= \frac{1 + \rho_c}{2}
 \end{aligned} \tag{13}$$

and its contrapositive

$$\tilde{\alpha}_c(\mathbf{x}) > \frac{1 + \rho_c}{2} \implies \alpha_c(\mathbf{x}) > \frac{1}{2}. \tag{14}$$

B. Additional Training Details

For CIFAR-10 and CIFAR-100, we perform ReCo at the 100th epoch and tune τ_{ps} for different noise rates. We show the values for τ_{ps} and λ_u in Tab. 7. We use smaller τ_{ps} for larger noise or more classes, as training with either of them decreases the confidence of the model. We set λ_r as 1 across all experiments. Choice of λ_u and λ_r follows (Li et al., 2020).

Dataset	CIFAR-10						CIFAR-100			
Noise type	Sym.			Asym.			Sym.			
Hyper-parameters \ Noise ratio	20%	50%	80%	90%	40%		20%	50%	80%	90%
τ_{ps}	0.9	0.9	0.8	0.8	0.8		0.8	0.8	0.5	0.3
λ_u	0	25	25	50	0		25	150	150	150

Table 7. Values of τ_{ps} and λ_u for different noise types and noise rates.

For Clothing1M and WebVision, we use the same hyper-parameters $\tau_{ps} = 0.8$, $\lambda_u = 0$ and $\lambda_r = 1$. We train the model for 100 epochs on both datasets, and perform ReCo at the 60th epochs. The warm up period is 1 epoch. We use SGD optimizer with a momentum of 0.8, a weight decay of 0.001, and a batch size of 32. For Clothing1M, the initial learning rate is set as 0.002 and reduced by a factor of 10 after 50 epochs. For WebVision, the initial learning rate is set as 0.01 and reduced by a factor of 10 after 50 epochs.

C. More Visualization

We show a complete distribution of all 10 classes of CIFAR-10 in Fig. 5. It can be seen from the figure that clusters learned by LC-Booster are more compact. Moreover, our method has fewer false predictions (marked as triangles) compared with DivideMix, showing its robustness under extreme label noise.

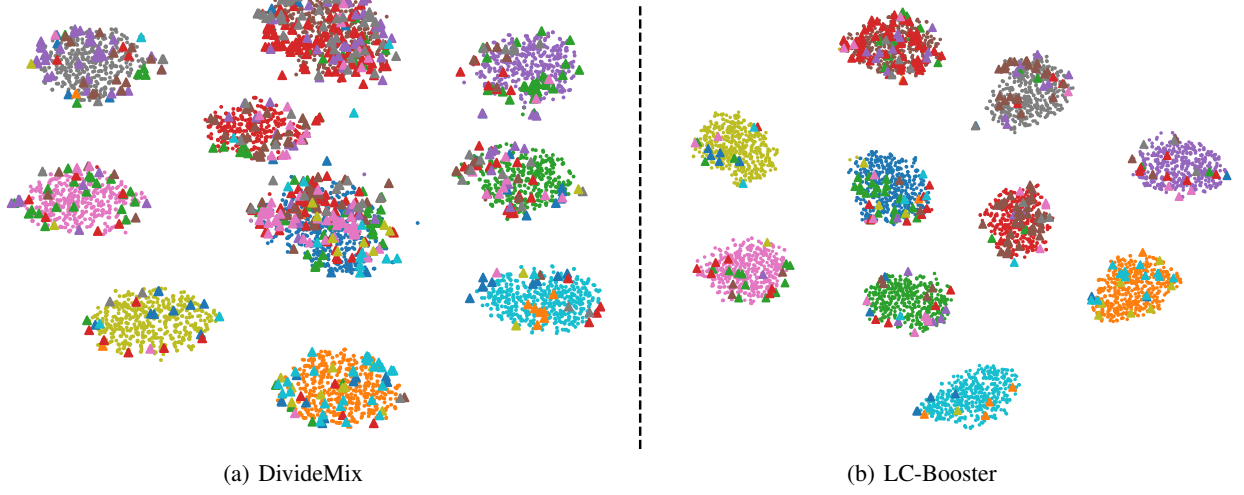


Figure 5. Visualization of embedded features on CIFAR-10 with 90% symmetric noise. 10 classes are visualized in different colors. Correct predictions are marked as circles and false predictions as triangles. Best viewed in color.

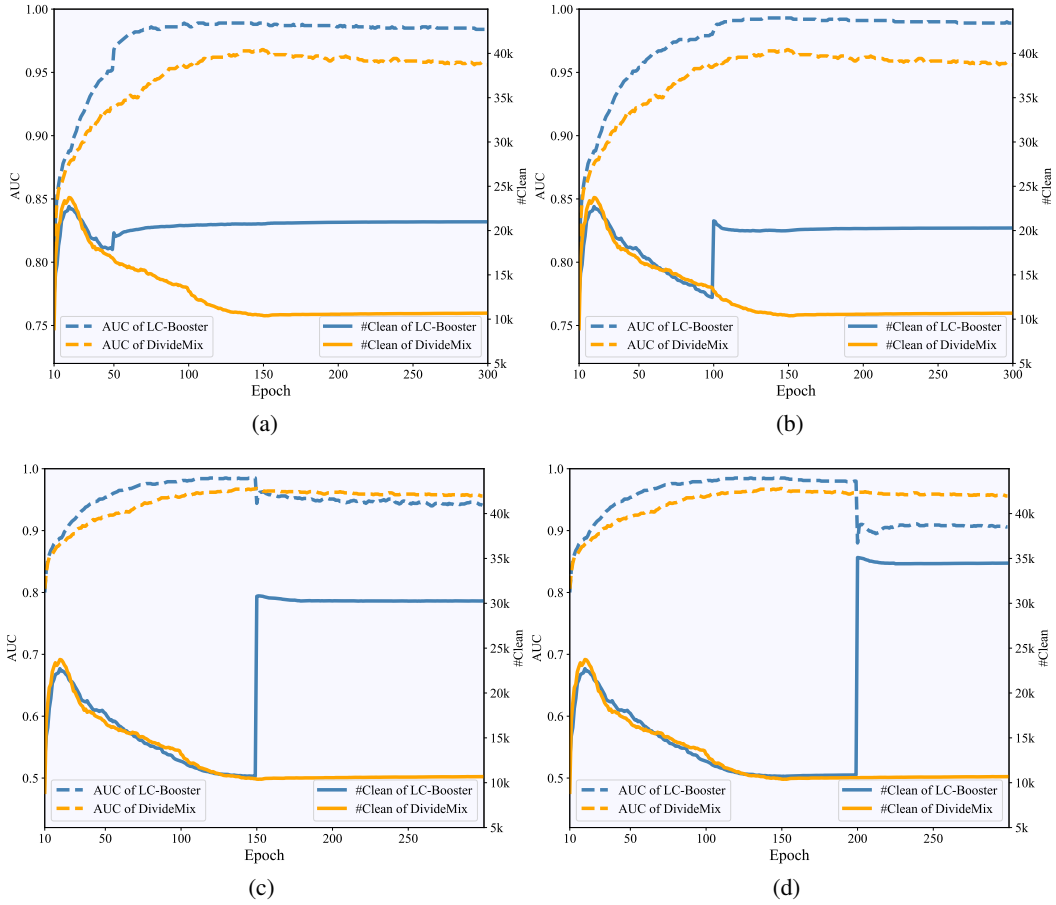


Figure 6. Curves of AUC and size of clean set (#Clean) on CIFAR-10 with 90% symmetric noise. Higher AUC indicates that clean samples are selected more precisely based on GMM. (a), (b), (c), (d) show the curves of performing ReCo at the 50th, 100th, 150th and 200th epoch, respectively.

We also show curves of AUC and size of clean set for different re-labeling epochs in Fig. 6. Re-labeling at the 100th achieves the highest AUC and the largest size. Earlier re-labeling at the 50th epoch may not be very much reliable, since the model has not been trained sufficiently. Re-labeling in later epochs (*e.g.*, the 150th and 200th epoch) results in a larger expansion of the clean set but a drop in AUC. We hypothesize this is due to overfitting to noisy samples.